

Supplemental Materials for

**Multiple bases of human intelligence revealed by cortical thickness
and neural activation**

Yu Yong Choi, Noah A. Shamosh, Sun Hee Cho, Colin G. DeYoung, Min Joo Lee,
Jong-Min Lee, Sun I. Kim, Zang-Hee Cho, Kyungjin Kim, Jeremy R. Gray*, Kun Ho Lee*

*To whom correspondence should be addressed. E-mail: leekho@snu.ac.kr or
jeremy.gray@yale.edu

This PDF file includes:

Supplemental Methods

Supplemental References

Supplemental Figures 1 to 5

Supplemental Tables 1 to 4

Supplemental Methods

Participants

Protocols were approved by the relevant institutional review boards (Seoul National University, Catholic University of Korea), and written informed consent was obtained from participants. 469 volunteers were recruited through advertisements and screened to cover the entire range of intelligence except the potentially retarded range. We tried to obtain an equal representation of subjects in all ranges such as average, high, and superior IQ by recruiting more subjects with superior IQ, because if we had only few data points at the extremes these might turn out to be outliers distorting the overall correlational relationships and making it difficult to satisfy the basic assumptions of regression analysis such as homoscedasticity. Finally, 225 healthy volunteers were retained with a wide distribution of WAIS full-scale IQs ($81 \leq \text{IQ} \leq 150$; supplemental Table 1): 122 male / 103 female, mean (SD) age = 20.9 (2.9) years, IQ = 118 (15). 164 and 109 subjects were scanned for anatomical and functional MRI data respectively, and forty eight of these subjects contributed both structural and functional samples (supplemental Table 1). Data from 33 subjects (functional sample) have been reported previously (Lee et al., 2006). For the structural sample, subjects were scanned at the Neuroscience Research Institute (NRI, Gachon University, Korea) or the Korea Advanced Institute of Science and Technology (KAIST, Korea). The two groups of subjects did not differ significantly in WAIS IQ and RPM scores [$t(162) < 0.24, p > .8$] or gender ratio ($\chi^2 = 1.10, p > .2$). Moreover, the correlations between WAIS IQ and cortical thickness at each surface point did not differ significantly between the NRI and

KAIST samples ($p > .001$ uncorrected; particularly in the ROIs, $p > .01$ uncorrected) based on the results of Fisher's z transformation analysis.

Psychometric Tests

All participants underwent both the Korean version of the Wechsler Adult Intelligence Scale-Revised (WAIS) and the Raven's Advanced Progressive Matrices Set II (RPM). The WAIS is a standard intelligence quotient (IQ) test that incorporates 11 subtests on diverse cognitive abilities: Information, Comprehension, Vocabulary, Similarities, Block Design, Object Assembly, Picture Completion, Digit Span, Arithmetic, Digit Symbol, and Picture Arrangement (Yum et al., 1992); it can provide individual levels of both crystallized intelligence (gC) and fluid intelligence (gF) (Marshalek et al., 1983). Factor analytical studies of WAIS have identified the presence of factors named Verbal Comprehension and Perceptual Organization, and demonstrated that Information, Comprehension, Vocabulary, and Similarities subtests are classified into strong measures of Verbal Comprehension or gC , and Block Design, Object Assembly, and Picture Completion subtests are categorized into strong measures of Perceptual Organization or gF (Beck et al., 1985; Leckliter et al., 1986; Marshalek et al., 1983; Parker, 1983). The RPM, a standard test for general intelligence, is one of the purest measures of psychometric g (Raven et al., 1998). In this study, g is the principal factor of RPM and all subtests of WAIS, gC is the principal factor of WAIS Verbal Comprehension subtests, and gF is the principal factor of WAIS Perceptual Organization and RPM.

Anatomical MRI Acquisition and Processing

At NRI, contiguous 0.9 mm axial MPRAGE images were acquired with a 1.5T MR scanner (Magnetom Avanto, Siemens) with TR=1160 ms; TE=4.3 ms; flip=15°; FOV=224 mm; matrix=512x512; number of slices=192; two images were acquired and averaged. At KAIST, MPRAGE images were obtained with a 3T MR scanner (Forte, Isol Technology) with TR=10 ms; TE=5.7 ms; flip=10°; FOV=220 mm; matrix=256x256; number of slices=128; slice thickness=1.5 mm. Anatomical images were corrected for intensity non-uniformity (Sled et al., 1998), spatially registered to stereotaxic space (Collins et al., 1994), and masked to remove extra-cerebral voxels. We used INSECT (Zijdenbos et al., 2002) to classify gray matter (GM), white matter (WM), and cerebrospinal fluid (CSF).

Cortical Thickness

Thickness measurement requires specific algorithms to reconstruct the inner and outer cortical surfaces (MacDonald et al., 2000). These surfaces are automatically reconstructed by the Constrained Laplacian-based Automated Segmentation with Proximities (CLASP) algorithm (Kim et al., 2005). CLASP extracts the inner cortical surface by deforming a sphere polygon model to the boundary between GM and WM. The number of triangles of the polygon model is hierarchically refined from 320 to 80920. Then, the outer cortical surface is expanded from the inner surface to the boundary between GM and CSF along a Laplacian map, which smoothly increases

potential surfaces between WM and CSF. A CSF fraction image is skeletonized to determine the boundary of the outer cortex in buried sulci. We constructed hemispheric cortical surface models, each of which consisted of 81,920 polygons forming high-resolution meshes of discrete triangular elements. Since the cortical surface models were extracted from MR volumes transformed into stereotaxic space, to measure cortical thickness in native space we applied an inverse transformation matrix to the cortical surfaces and reconstructed them in native space. The inner and outer surfaces had the same vertex number (40962), and the correspondence of each vertex between surfaces was defined in the reconstruction process. Thus, cortical thickness was easily measured using the t-link method of calculating the Euclidean distance between linked vertices on the white matter surface and the GM/CSF intersection surface (Kabani et al., 2001).

fMRI Experiments

The tasks requiring fluid reasoning ability and the functional MRI protocol were as described elsewhere (Lee et al., 2006). Significant clusters of activation correlated with WAIS IQ were used as the region of interest (ROI), with height ($p < .001$ uncorrected) and extent ($p < .05$ uncorrected) thresholds. For each ROI, we averaged the 10 voxels with the highest t-scores from a contrast of complex reasoning > simple reasoning. For figure production, we used FreeSurfer (CorTechs Labs Inc., Charlestown, MA) and SPM surfrend toolbox (<http://spmsurfrend.sourceforge.net>).

Statistical Analysis

In the CLASP algorithm, every vertex has the thickness information on the cortical surface. To compare thickness across subjects, the thickness information was spatially normalized. The vertices were transformed to the spherical model from which the cortical surfaces originated, and nonlinearly registered to an average template on the sphere. A highly flexible deformation, in two dimensions, of a template cortex to an individual was used for cortical surface registration. This algorithm provided a transformation to match crowns of gyri between subjects using a geodesic distance map. With this transformation, thickness information on the vertices was transformed to a template. Then, diffusion smoothing, which generalizes Gaussian kernel smoothing, with 30 mm FWHM (full width half maximum) was used to increase the signal to noise ratio (Chung et al., 2003).

Statistical parametric maps of the cortical correlates of intelligence were constructed using Pearson's correlation. The distribution of thickness across the whole brain was assessed initially on a vertex-by-vertex basis. When the NRI and KAIST data were combined, to reduce variation caused by different scanner characteristics, the KAIST data were used after normalizing the distribution of the thickness at each cortical surface location on the basis of the NRI data. The normalization procedure equalized the means and the standard deviations of two datasets by multiplying each z value from KAIST data by the standard deviation of NRI data and then adding it with the mean of NRI data. Cortical areas correlated to WAIS IQ were used as the region of interest with statistical significance ($p < .001$, uncorrected). For each ROI, we averaged the 10 surface points with the greatest thicknesses.

Supplemental References

- Beck NC, Horwitz E, Seidenberg M, Parker J, Frank R (1985) WAIS-R factor structure in psychiatric and general medical patients. *J Consult Clin Psychol* 53:402-405.
- Chung MK, Worsley KJ, Robbins S, Paus T, Taylor J, Giedd JN, Rapoport JL, Evans AC (2003) Deformation-based surface morphometry applied to gray matter deformation. *Neuroimage* 18:198-213.
- Collins DL, Neelin P, Peters TM, Evans AC (1994) Automatic 3D intersubject registration of MR volumetric data in standardized Talairach space. *J Comput Assist Tomogr* 18:192-205.
- Kabani N, Le Goualher G, MacDonald D, Evans AC (2001) Measurement of cortical thickness using an automated 3-D algorithm: a validation study. *Neuroimage* 13:375-380.
- Kim JS, Singh V, Lee JK, Lerch J, Ad-Dab'bagh Y, MacDonald D, Lee JM, Kim SI, Evans AC (2005) Automated 3-D extraction and evaluation of the inner and outer cortical surfaces using a Laplacian map and partial volume effect classification. *Neuroimage* 27:210-221.
- Leckliter IN, Matarazzo JD, Silverstein AB (1986) A literature review of factor analytic studies of the WAIS-R. *J Clin Psychol* 42:332-342.
- Lee KH, Choi YY, Gray JR, Cho SH, Chae JH, Lee S, Kim K (2006) Neural correlates of superior intelligence: Stronger recruitment of posterior parietal cortex. *Neuroimage* 29:578-586.
- MacDonald D, Kabani N, Avis D, Evans AC (2000) Automated 3-D extraction of inner and outer surfaces of cerebral cortex from MRI. *Neuroimage* 12:340-356.
- Marshalek B, Lohman DF, Snow R (1983) The complexity continuum in the radex and hierarchical models of intelligence. *Intelligence* 7:107-127.
- Parker K (1983) Factor analysis of the WAIS-R at nine age levels between 16 and 74 years. *J Consult Clin Psychol* 51:302-308.

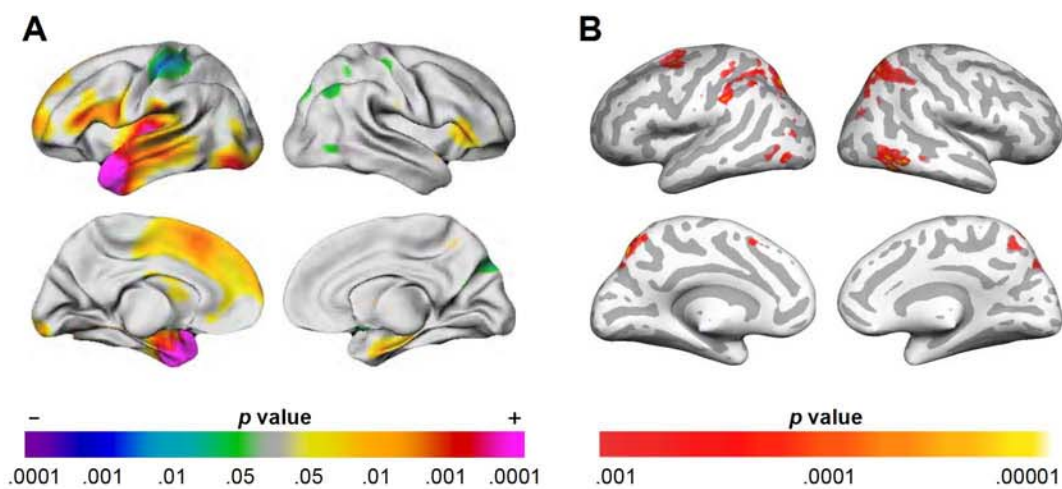
Raven J, Raven JC, Court JH (1998) Manual for Raven's Progressive Matrices and Vocabulary Scales. Oxford: Oxford Psychologists Press.

Sled JG, Zijdenbos AP, Evans AC (1998) A nonparametric method for automatic correction of intensity nonuniformity in MRI data. IEEE Trans Med Imaging 17:87-97.

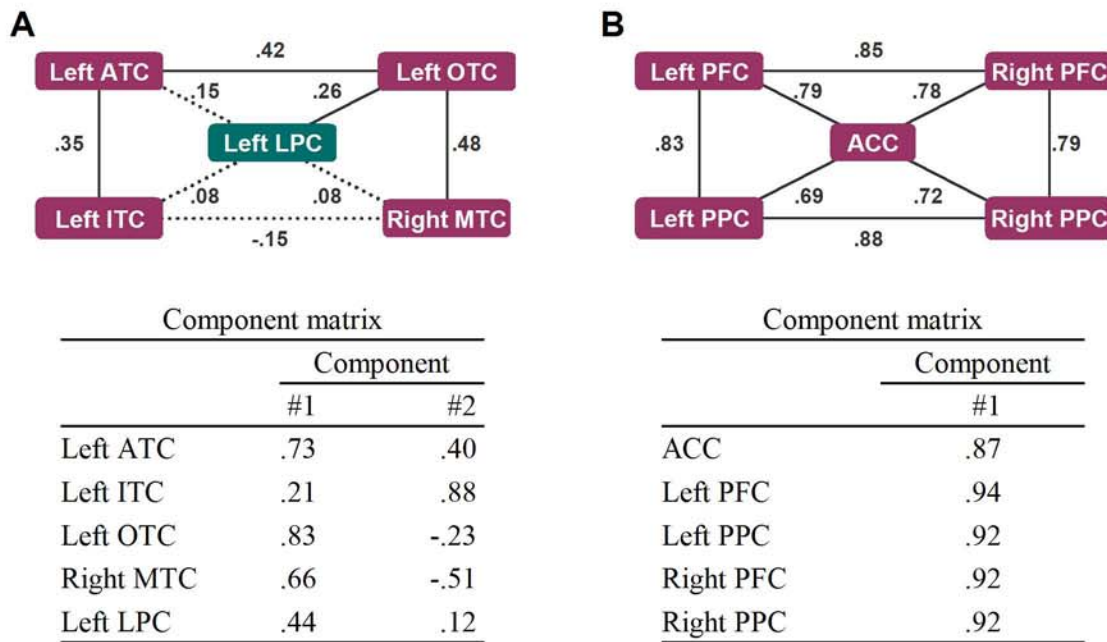
Yum TH, Park YS, Oh KJ, Kim JK, Lee YH (1992) Korean Wechsler Adult Intelligence Scale (K-WAIS) manual. Seoul: Handbook Guidance.

Zijdenbos AP, Forghani R, Evans AC (2002) Automatic "pipeline" analysis of 3-D MRI data for clinical trials: application to multiple sclerosis. IEEE Trans Med Imaging 21:1280-1291.

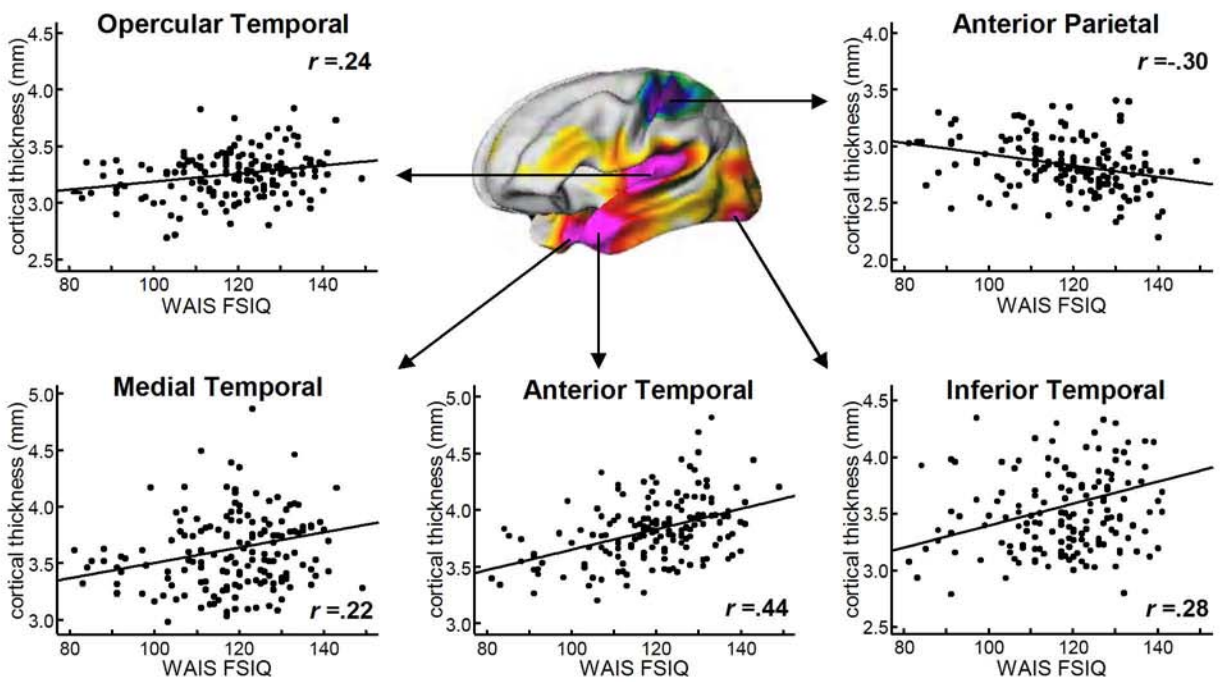
Supplemental Figures



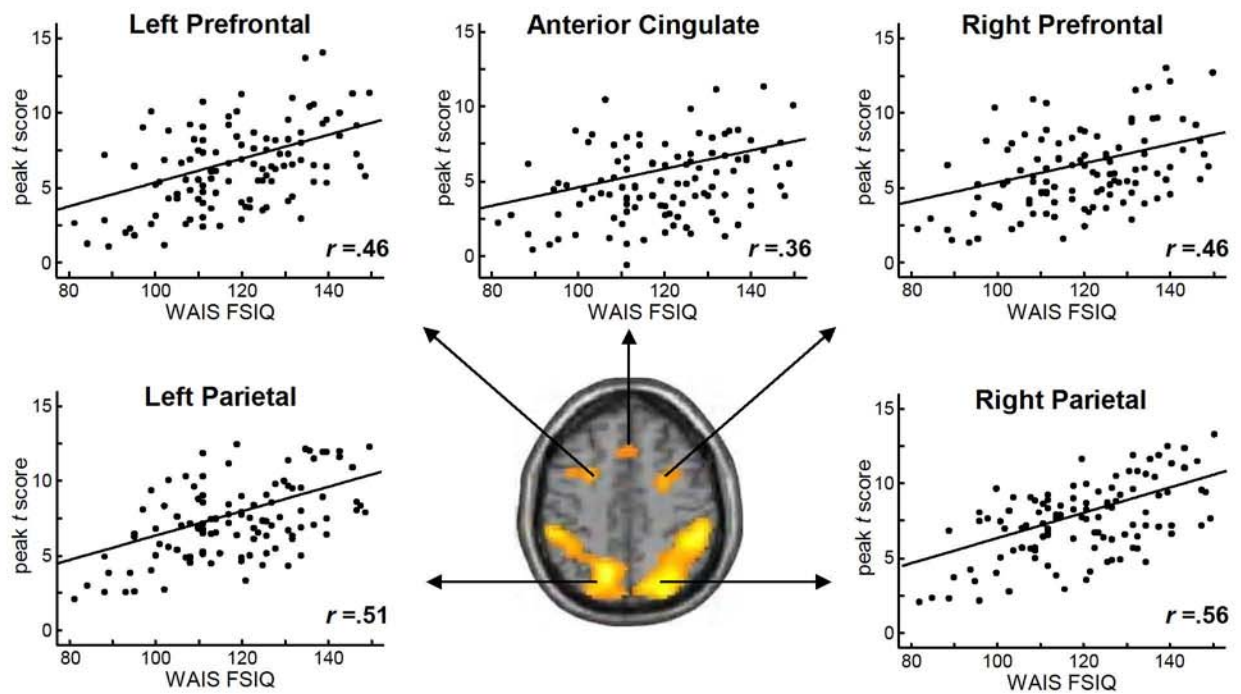
Supplemental Figure 1. Correlations between cortical gray matter thickness (**A**) or cortical activation during reasoning tasks (**B**) and RPM scores. The color bars indicates statistical significance of the correlations. In panel A, the left side of the color bar shows the negative correlation and the right side the positive correlation.



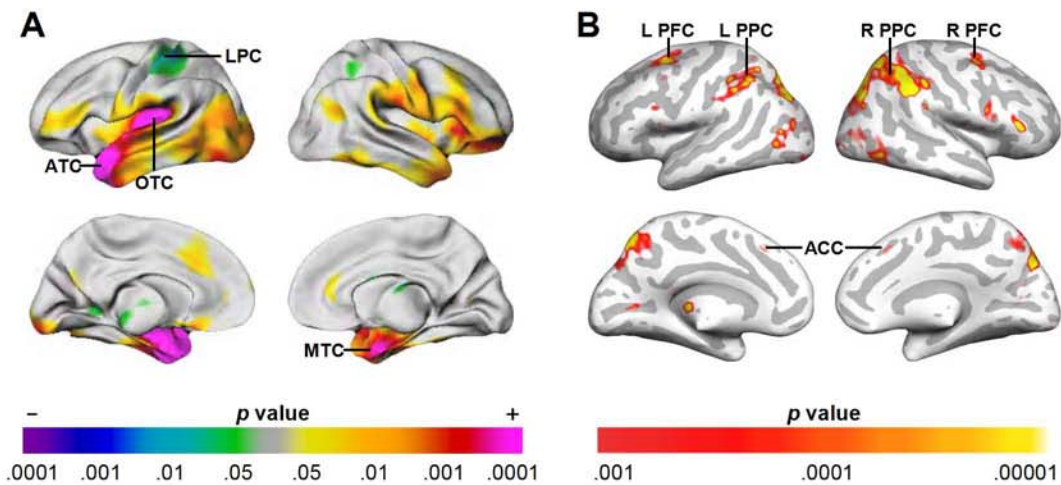
Supplemental Figure 2. Inter-correlations and principal component analysis of the structural ROIs (**A**) and of the functional ROIs (**B**). Each value on a line indicates the correlation coefficient between the connected ROIs. The statistical significance is denoted by a solid ($p < .05$) or dashed ($p > .05$) line. The positive correlates with psychometric scores were boxed in purple, whereas the negative correlate was boxed in green. The results of the principal component analysis, the component matrices, show that there were two components with eigen values > 1 in the structural and one in functional ROIs. LPC, lateral parietal cortex; ATC, anterior temporal cortex; ITC, inferior temporal cortex; MTC, medial temporal cortex; ACC, anterior cingulate cortex; PFC, prefrontal cortex; PPC, posterior parietal cortex.



Supplemental Figure 3. Scatter plots and linear regression lines showing the relationship between the cortical gray matter thickness of each ROI and FSIQ score. The ROIs were defined by the correlations between cortical thickness and FSIQ ($p < .001$ uncorrected).



Supplemental Figure 4. Scatter plots and linear regression lines showing the correlation between cortical brain activation in each ROI and FSIQ score. The ROIs are defined by a simple regression analysis with FSIQ score as a covariate ($p < .001$ uncorrected).



Supplemental Figure 5. Structural (**A**) and functional (**B**) ROIs for a neurometric IQ model. The ROIs were newly defined within the anatomical dataset ($n = 116$, $p < .001$) and within the functional dataset ($n = 61$, $p < .001$). The color bars indicate statistical significance of the correlations. In panel A, the left side of the color bar shows the negative correlation and the right side the positive correlation.

Supplemental Tables

Supplemental Table 1. Subject information and behavioral data

	Whole sample	Type of imaging modality	
		Anatomical MRI	Functional MRI
Participant (M/F)	$n = 225$ (122/103)	$n = 164$ (89/75)	$n = 109$ (62/47)
Age	20.9 ± 2.9	21.6 ± 2.5	20.1 ± 2.8
Psychometric tests			
WAIS FSIQ	119 ± 15	119 ± 14	119 ± 16
RPM score	28.1 ± 6.0	28.2 ± 5.9	28.3 ± 6.5

Forty eight subjects provided both anatomical and functional MRI data. All data are *Means* \pm *SD*. M, male; F, female.

Supplemental Table 2. Relationships between intelligence measures and structural or functional ROIs

Score	Structural ROI (correlation coefficient)						Functional ROI (correlation coefficient)					
	All	ATC	ITC	OTC	MTC	LPC	All	ACC	LPFC	LPPC	RPFC	RPPC
WAIS	.63	.44	.28	.24	.22	-.30	.56	.36	.46	.51	.46	.56
RPM	.50	.40	.20	.19	.09	-.22	.57	.32	.44	.53	.43	.54

The correlation coefficients were calculated between intelligence scores and regional peak thickness (for structural ROIs) or peak *t* scores (for functional ROIs). The columns named “All” give the multiple correlation coefficients between the five ROI values and the intelligence scores. ATC, anterior temporal cortex; ITC, inferior temporal cortex; MTC, medial temporal cortex; OTC, opercular temporal cortex; LPC, lateral parietal cortex. ACC, anterior cingulate cortex; PFC, prefrontal cortex; PPC, posterior parietal cortex; L, left; R, right.

Supplemental Table 3. Correlation coefficients between regional thickness and Verbal or Performance scores

Test	Correlation coefficient (<i>r</i>)				
	ATC	ITC	OTC	MTC	LPC
Verbal IQ	.43**	.30**	.24*	.24*	-.33**
Information	.36**	.23*	.21*	.16	-.31**
Comprehension	.37**	.23*	.22*	.20	-.22*
Vocabulary	.31**	.15	.19	.23*	-.30**
Arithmetic	.41**	.30**	.13	.18	-.30**
Similarities	.22*	.28**	.15	.13	-.33**
Digit span	.28**	.20*	.16	.15	-.16
Performance IQ	.36**	.20*	.20*	.15	-.18
Picture completion	.15	.09	.16	.06	-.08
Picture arrangement	.29**	.14	.08	.11	-.08
Digit symbol	.14	.10	.07	.08	-.18
Block design	.29**	.22*	.19	.08	-.16
Object assembly	.24*	.15	.06	.06	-.11

Each value is a Pearson correlation coefficient between the cortical thickness of the intelligence-related regions and the scores of WAIS Verbal and Performance tests. ATC, anterior temporal cortex; LPC, lateral parietal cortex; OTC, opercular temporal cortex; ITC, inferior temporal cortex; MTC, medial temporal cortex. *, $p < .01$; **, $p < .001$.

Supplemental Table 4. Behavioral information on the three groups based on intelligence levels as measured by major cognitive tests

	Group		
	Average IQ	High IQ	Superior IQ
Participant (<i>n</i>)	54	55	55
<i>Score</i>			
VIQ (rank)	101 ± 8 (53%)	118 ± 4 (88%)	133 ± 6 (99%)
PIQ (rank)	102 ± 9 (55%)	118 ± 2 (88%)	128 ± 5 (97%)
FSIQ (rank)	103 ± 9 (58%)	120 ± 3 (91%)	132 ± 5 (98%)
RPM (rank)	21.3 ± 4.1 (54%)	29.2 ± 1.6 (86%)	33.9 ± 1.3 (99%)
<i>Age</i>			
VIQ	21.1 ± 2.8	22.4 ± 1.9	21.4 ± 2.6
PIQ	21.6 ± 2.6	22.3 ± 2.3	21.0 ± 2.4
FSIQ	21.5 ± 2.6	22.3 ± 2.4	21.2 ± 2.4
RPM	21.7 ± 3.0	22.4 ± 2.3	20.9 ± 2.0
<i>Gender ratio (M/F)</i>			
VIQ	28/26	31/24	30/25
PIQ	27/27	30/25	32/23
FSIQ	27/27	28/27	34/21
RPM	30/24	25/30	34/21

Scores and ages present in $M \pm SD$. Rank gives the percentile rank of each mean score. M, male; F, female.